Programmable Writing of Graphene Oxide/Reduced Graphene Oxide Fibers for Sensible Networks with *in Situ* Welded Junctions

Jun Cao,[†,‡,∥] Yongyi Zhang,[†,∥] Chuanling Men,[‡] Yanyan Sun,[†,§] Zhaona Wang,[§] Xuetong Zhang,[†,⊥,*] and Qingwen Li[†,*]

[†]Suzhou Institute of Nano-Tech & Nano-Bionics Chinese Academy of Sciences, Suzhou 215123, P. R. China, [‡]School of Energy and Power Engineering, University of Shanghai for Science and Technology, Shanghai 200093, P. R. China, [§]Department of Physics Beijing Normal University, Beijing 100875, P. R. China, and [⊥]School of Materials Science & Engineering Beijing Institute of Technology, Beijing 100081, P. R. China. [∥]These authors contributed equally to this work.

ABSTRACT Direct spinning of the graphene oxide (GO) dispersions from a moveable spinneret along the programmed track, *i.e.*, a "programmable writing" technique, was developed to make nonwoven, nonknitted, graphene-based networks with excellent mechanical properties. The resulting GO networks can be successfully converted into reduced GO (RGO) ones with better mechanical properties as well as excellent electrical conductivity *via* thermal/chemical reduction. *In situ* welded junctions formed during processing of the spun fibers have made the resulting networks with the integral structure, and outstanding mechanical properties and high electrical conductivities of the spun fibers and their web integrations have provided a great opportunity to remotely sense the external mechanical stimuli *via* electrical signal monitoring.

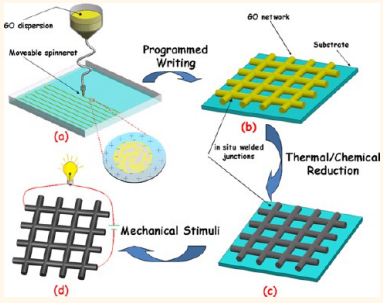

KEYWORDS: graphene oxide · graphene · networks · programmable writing · junctions

Standard two-dimensional (2D) electronic textiles (e-textiles), also known as intelligent textiles or smart ones, is a novel type of high-tech products resulting from the integration of electronics and textiles or clothing.[1,2] Smart textile systems span the range of applications including agro-textiles, energy, telecommunications, displays, *etc.*[2−7] Conventional smart textiles can be made by weaving or knitting of the insulating fibers and other fibers with additional functions (*e.g.*, electrical or optical conductivity) together.[8] Weaving is a process that interlaces two perpendicular sets of yarns, while knitting is a method in which yarns are arranged into consecutive loops (stitches) on a knitting needle. Both knitted and woven smart textiles are mechanics strong and deformation resistant, but the processing procedures are more complicated and facility costs are higher in comparison with either nonwoven or nonknitted textile fabrics. Furthermore, conductive fibers and their 2D frameworks within smart textiles are of particular interest for textile integration,[5,9] but either woven or knitted processing of these conductive fibers can only provide interconnects with limited conductivity as large contact resistance has existed between the interconnected fibers. Therefore, nonwoven, nonknitted smart textiles with high mechanical performance, high deformation resistance, and high electrical conductivity are highly desirable for the next generation applications.

Graphene, the first 2D nanostructure with superior electrical, mechanical, and optical properties,[10−19] is expected to serve as lightweight, highly conductive nanobuilding blocks for the flexible textiles. Graphene oxide (GO), a single sheet of graphite oxide, is an intermediate during wet chemistry synthesis of graphene *via* the method of oxidation−exfoliation−reduction of graphite powder.[11,20−22] It has been reported that macroscopic graphene-based woven fabrics or networks have been directly fabricated by chemical vapor deposition (CVD);[23−25] however, this process suffers from high temperature and substrate-etching, and thus limits its

* Address correspondence to zhangxtchina@yahoo.com, qwli2007@sinano.ac.cn.

Received for review November 17, 2013 and accepted April 7, 2014.

Published online April 07, 2014
10.1021/nn4059488

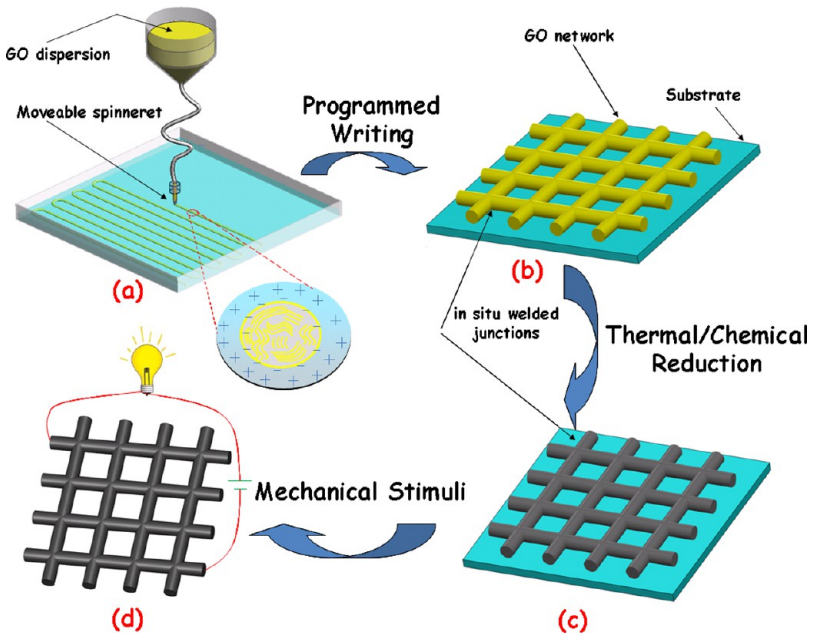

Figure 1. Programmable writing of GO/RGO fibers for sensible networks: (a) schematic diagram for the programmable writing of the graphene-based 2D networks with graphene oxide (GO) inks from a moveable spinneret; (b) the resulting GO networks with *in situ* welded junctions on the substrate; (c) the corresponding reduced graphene oxide (RGO) network made by thermal or chemical reduction of the resulting GO network; and (d) brightness of the bulb connected to the RGO networks changing with the pulsed mechanical stimulus, indicative of the sensible attribute of the resulting RGO networks.

large-scale applications. This has driven researchers to develop superior strategies to make the graphene-based networks *via* the following steps:[26,27] (1) wet spinning of GO fibers from a fixed-position spinneret, (2) weaving or knitting of the as-made GO fibers into the corresponding networks, and (3) converting of the GO networks into graphene ones by using thermal or chemical reduction. According to this strategy, the resulting 2D webs with mechanically strong, electrically conductive fibrous graphene building blocks have been obtained,,[26−28] however, fiber spinning from fixed-position spinneret has had the result that the weaving or knitting is an absolutely necessary step for the resulting graphene-based networks (*i.e.*, lack of programming power to directly make graphene-based complex structures with the spun GO fibers), and that the interconnected junctions among the graphene fibers are extremely weak in mechanics and ultralow in conductivity in comparison with the fibrous building blocks themselves, as weaving or knitting process cannot provide the most intimate connection, which might cause serious problems when these graphene-based webs were embedded in the insulating fabrics. For instance, the graphene-based networks with mechanically weak interconnections could be disconnected when the whole fabric was subjected to random mechanical forces, while the poor conductivity existed in the junctions of the networks could be easily fused when the current passes through and could cause slow response when external stimuli have been applied. These serious problems would lead to the performance of the resulting e-textiles not meeting the practical requirement, and thus, the novel strategies have to be developed as soon as possible to provide the solutions for such severe problems.

Herein, we have presented a "programmable writing" technique to make nonwoven, nonknitted, graphene-based networks by direct spinning of the GO dispersions from a moveable spinneret along the programmed track. The resulting GO networks with excellent mechanical properties have been successfully converted into reduced GO (RGO) networks with better mechanical properties as well as excellent electrical conductivity. The joint points formed by *in situ* welded effect have made the graphene-based networks with integral structures, in which the sufferable shear force of the junction is at least twice as high as that of the fiber. High electrical conductivity combining with outstanding mechanical flexibility has provided a facile way for RGO fibers and their web integrations to sense external mechanical stimuli by using electrical signals. The work presented here, to the best of our knowledge, is the first report on the programmable spinning of the graphene-based networks from the moveable spinneret, and *in situ* welded junctions among interconnected graphene-based fibers are the first observations among the graphene-based hierarchical assemblies. Our work also gives much inspiration to directly write any other complex networks based on various nanoscale building blocks as writable inks.

RESULTS AND DISCUSSION

Programmable writing of GO/RGO fibers for sensible networks is illustrated in Figure 1. Viscous GO dispersion

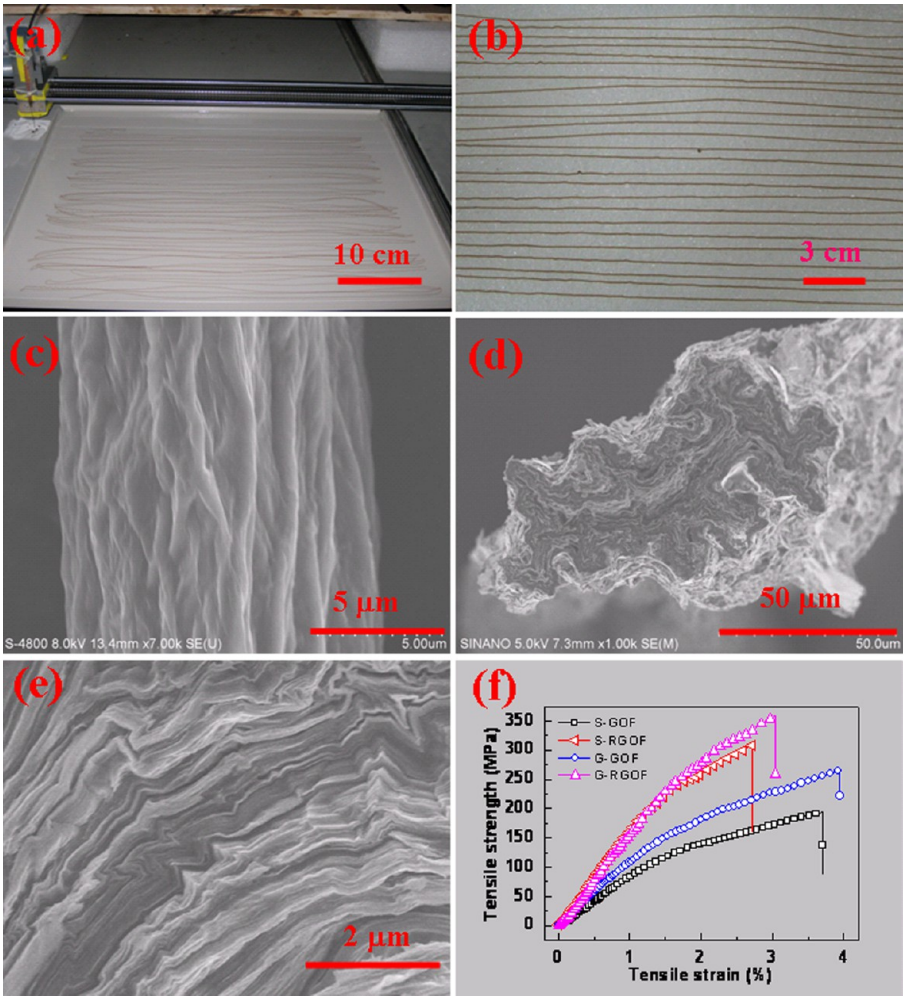

Figure 2. Directing writing of GO fibers: digital photos of the ultralong (tens of meters, a) and aligned (b) GO fibers, SEM images of the surface (c) and cross section (d and e) of the resulting GO fibers, and stress−strain curves (f) of the resulting GO and RGO fibers.

was filled in the pen-like injection syringe, which was fixed to a motor as shown in Figure 1a. GO sheets could be considered as negatively charged macromolecules due to ionization of carboxylic acid groups at the edges of the sheets.[29−31] When the GO dispersion was injected into the coagulation bath containing oppositely charged molecules (*e.g.*, cetyltrimethylammonium bromide (CTAB), multivalent metal ions, *etc.*), there was interfacial self-assembly between the negatively charged GO sheets and positively charged coagulation molecules at the beginning,[32,33] and then the sheets curled and folded into a fibrous structure. By controlling the motor that moves the injection syringe along the predetermined track, we could easily obtain GO 2D-web at the bottom of the coagulation bath as shown in Figure 1b. The way we make GO 2D-web here is quite similar as the way people write with the usual inks on blank paper, so we call it "direct writing with GO ink". After step of purification, ambient drying, and thermal/chemical reduction of the GO 2D-web in sequence, the resulting RGO 2D network was successfully obtained as shown in Figure 1c. The sensing ability of the resulting RGO network was reflected in changing brightness of the bulb connected to the RGO networks with the pulsed mechanical stimulus as illustrated in Figure 1d.

First, the capability of direct writing with GO dispersion, as illustrated in the making of GO fibers as shown in Figure 2, has been further investigated in detail. Ultralarge GO sheets were synthesized according to modified Hummers' method without ultrasonic treatment.[11] The thickness of GO sheet measured by atomic force microscopy was ~0.8 nm (Figure S1), indicating the monolayer attribute of obtained GO sheets existed in water.[22] The average lateral size of the GO sheets was 30 μm with a relatively wide distribution (Figure S2) ranging from dozens of micrometers (up to 102 μm) to several micrometers (down to 5 μm). Relatively small GO sheets with the average lateral size of 17 μm (Figure S3) were easily obtained from large GO sheets by using ultrasonication. Both GO sheets with above different lateral sizes could be used as the GO inks in our direct writing for fibers. However, when further decreasing the lateral size of GO sheets down to *ca.* 35 nm, we can

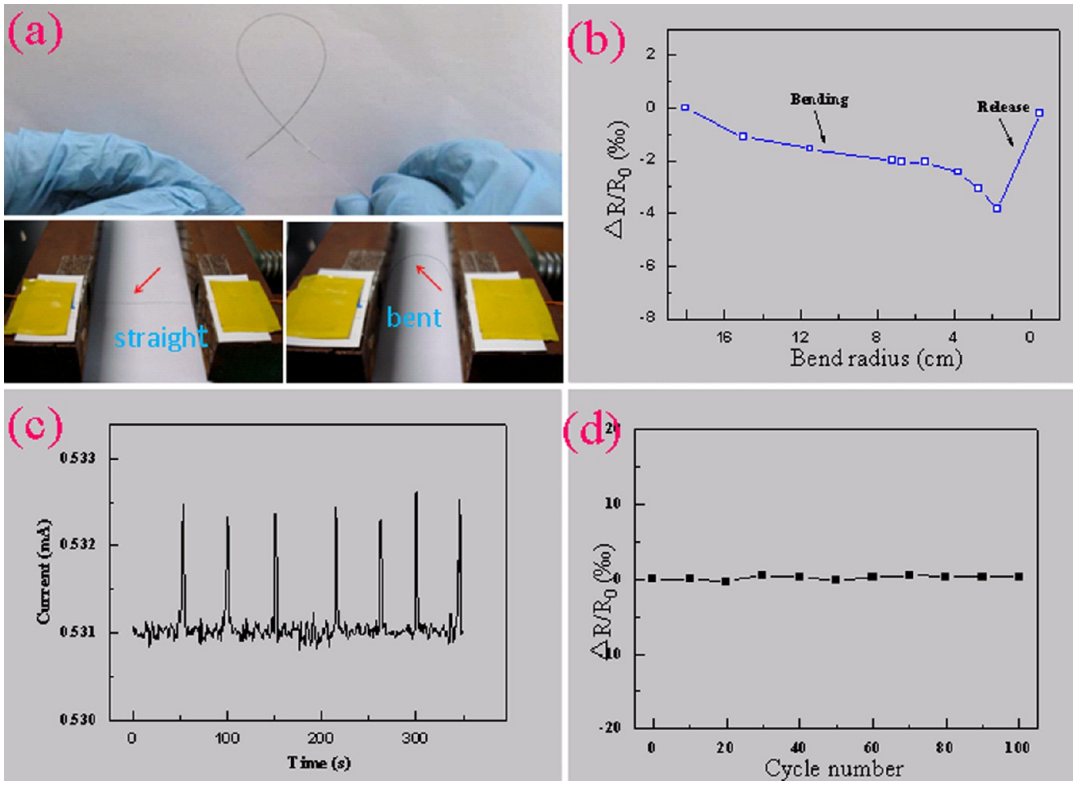

Figure 3. The changes of the electrical signals with the mechanical stimuli: (a) digital photo of the bent RGO fibers held by two hands; (b) the relationship between the relative resistance change and the bent radium; (c) the current pulse under the bent status of the RGO fiber; and (d) cyclic stability of the RGO fibers under the repeated bending. Insets in (a) are the real recording photos on how to measure the resistance−strain curves for the obtained RGO fibers.

still perform direct writing of GO fiber from the spinneret, but cannot draw it from coagulating bath and it breaks into pieces (Figure S4). These investigations have indicated that the capability of the direct writing with GO sheets is size-independent in the range of several tens of nanometers to several tens of micrometers. Actually, GO viscosity (higher than 3 Pa·s) is a key factor to determine whether successive fibers could be successfully written out as shown in Figure S5 (and thus to affect the microstructure of the resulting GO fibers as shown in Figure S6), which indicated that the capability of the direct writing with GO dispersions is viscosity-dependent.

Ultralong (tens of meters) GO fibers without breakage and with swerves at each end of the bath container perpendicular to the moving direction of the motor could be written out continuously in the CTAB coagulation bath as shown in Figure 2a. By controlling the movement of injection syringe, we could get GO fibers with parallel alignment as shown in Figure 2b. Similarly, by adjusting the needle diameter, injecting rate, and writing speed during the direct writing process, we could get the GO fibers with various sizes in diameter ranging from a dozen micrometer to hundreds of micrometers (Figure S7). The surfaces of the GO fibers show uniform alignment of wrinkles along the axis (Figure 2c) caused by the dehydration-responsive shrinkage during drying process.[34,35] The morphology observation at the cross section of the fibers has revealed that the assembled GO sheets are stacked compactly in layers with some degree of dentate folding (Figure 2d), and closer observation has indicated that the GO building blocks are stacked together to form densely ordered lamellar microstructures with waved morphology (Figure 2e).

For the GO dispersion with the same viscosity (50 Pa·s), the tensile strength of the fibers (G-GOF) assembled by the GO sheets with lateral size of 30 μm is 267 MPa (Figure S6) with a Young's modulus of 14 GPa, which is much stronger in comparison with those of fibers (S-GOF) assembled by the GO sheets with the lateral size of 17 μm (192 MPa and 11 GPa, respectively) due to the size-induced enhancement.[35−38] In addition, the tensile strengths of the resulting GOFs have slightly changed with the viscosity of the GO inks (Figure S6), probably indicating that the different GO phases have been formed before direct writing.[28] Actually, these mechanical properties are very competitive to the results reported elsewhere.[35,39] The compact internal structure of the resulting GO fibers has leaded to their excellent mechanical properties. After chemical reduction by using hydroiodic acid,[35] the morphology of the surface and cross section of the GO fibers was preserved (Figure S6) and the mechanical performance of the resultant RGO fibers has been further enhanced as shown in Figure 2f. Specifically,

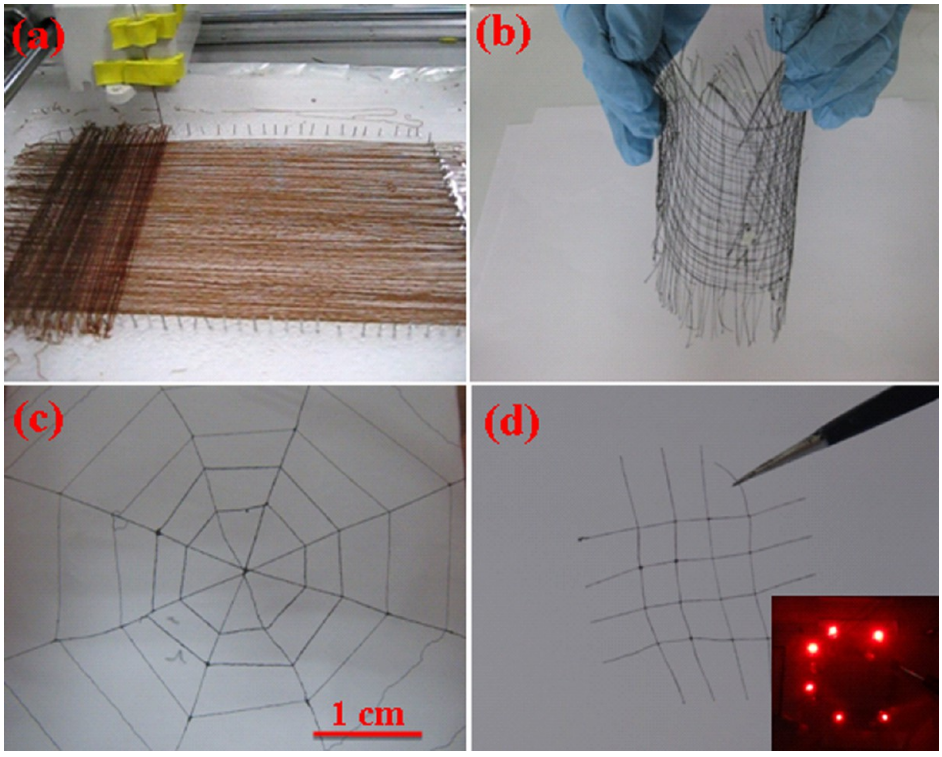

Figure 4. Digital photos of programmable writing of GO networks: (a) the writing of the longitudinal fiber array in the presence of the latitudinal fiber array; (b) the bent GO network on two hands; (c) the spider web-like GO network; and (d) the obtained RGO network held by a tweezer. Inset in (d) is the lighting of the LED bulb by using the RGO network as the conducting channel.

the G-GOF after reduction has a tensile strength of 365 MPa and a Young's modulus of 21 GPa, which are 37% and 50% higher than those of the original G-GOFs, respectively, due to the stronger interactions existing between the compact RGO sheets, resulting from partial removing of the oxygen-containing groups. The Raman spectra of GO and RGO fibers were shown in Figure S8c. The GO fiber has characteristic peaks at 1582 cm^{-1}(G-band) and 1355 cm^{-1} (D-band). The obvious band shifts and the increase in I_D/I_G ratio after chemical treatment have confirmed reduction of GOFs. The X-ray diffraction peak of GOFs at $2\theta = 11°$ means an interlayer spacing of 0.804 nm. After reduction, due to partial removal of the oxygen-containing groups, the interlayer spacing of graphene sheets got smaller, which was reflected in the new diffraction peak at $2\theta = 24.1°$ as shown in Figure S8d. The EDX spectra of the surface and cross section of the GO and RGO fibers were shown in Figures S9 and S10, respectively. We can see that surface oxygen contents have decreased from 20.87% to 7.15%, and the percentage reduction in oxygen arrives at 65.7%. However, the percentage reduction of the oxygen located at the cross section of the fiber has only reached 47%. The difference in oxygen percentage reduction between the surface and cross section is mainly due to the difference in microstructure. The oxygen groups located at the cross section area are much more difficult to be reduced in comparison with those located at the surface area.

The obtained RGO fibers after reduction exhibit high electrical conductivity and outstanding mechanical flexibility. The electrical conductivity of the G-RGOF is 2.7×10^4 s/m, while that of the S-RGOF is 1.8×10^4 s/m (see Figure S11), and reasons for the difference in conductivity are probably ascribed to the larger flake size and therefore less junction resistance in the G-RGO *versus* the S-RGO, as well as to different degrees of the RGO sheet orientation and internal packing defects.[35,40] The electrical conductivities of the resulting RGO fibers are comparable to the results reported elsewhere.[34,39,41] The obtained RGO fibers can be easily bent with a certain curvature as illustrated in Figure 3a, indicating the mechanical flexibility. High electrical conductivity combined with outstanding mechanical flexibility has provided a facile way for RGO fibers to sense external mechanical stimuli by using the changing electrical signals. As shown in Figure 3b, the electrical resistance changes of RGO fibers were small but obvious and monotonic when it was bent at a certain range of bending radius, which may be attributed to increasing "touch point" of the inner RGO sheets of the fibers.[23,42] To further demonstrate the electrical sensitivity and excellent detectability of our RGO fibers, we have recorded current-changes of the fibers with a fixed bending radius (3 cm) every 50 s as shown in Figure 3c, and observed regular current pulse signals when the bending was applied. After 100 bending−releasing cycles with a bending radius of 3 cm, the electrical

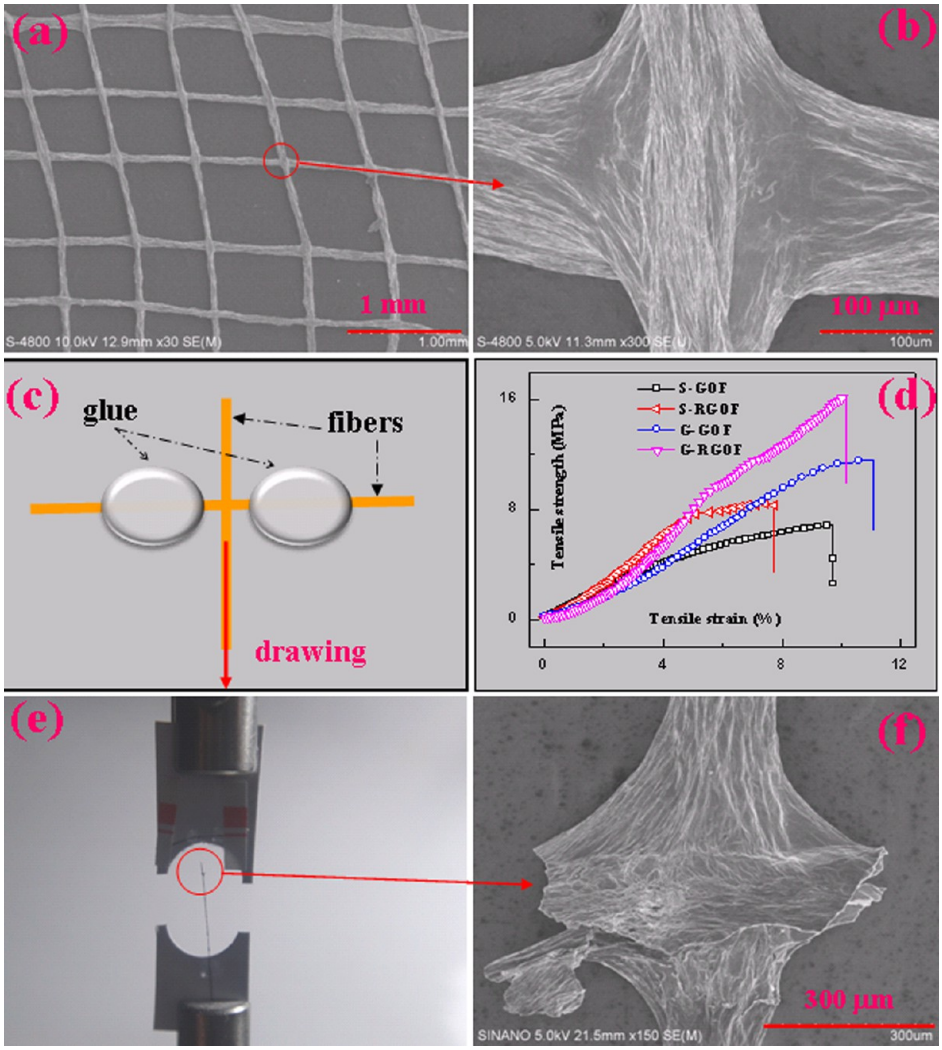

Figure 5. Illustration of the *in situ* welded junctions within the written graphene-based network: SEM images of the formed junctions with low (a) and high (b) magnifications; the schematic picture on how to apply the load to an *in situ* welded junction (c); stress–strain curves of various junctions existing in the graphene-based network (d); digital photo (e) and SEM image (f) of one broken junction after applying the load.

resistance remains constant as shown in Figure 3d (finally the resistance only changes ~1.5 and the maximum change is below 3), indicating an excellent mechanical stability.

Direct writing with GO inks has provided an extremely powerful strategy to make programmable 2D patterns (*i.e.*, webs) at the bottom of the coagulation bath. In virtue of the moveable "pen nib", we can directly write a parallel GO fiber array at the bottom of the coagulation bath along the latitudinal direction, and then we can immediately write another parallel GO fiber array at the bottom of the coagulation bath along the longitudinal direction (Figures 4a and S12). The existence of the latitudinal array cannot influence the writing of the longitudinal array, and there are a lot of junctions (in other word, 2D network) formed between the latitudinal and longitudinal arrays. Obviously, neither weaving nor knitting has been used for these 2D webs owing to programmable writing with GO inks and moveable nib. The written GO network with mutual perpendicular fiber arrays has shown excellent flexibility after coagulation, washing, and drying of the obtained structure in sequence (Figure 4b). Most importantly, the directly written GO webs can be easily converted into RGO webs only *via* chemical or thermal reduction, and the resulting RGO 2D webs have not only preserved the flexibility of the GO 2D-web (Figure S13), which can be confirmed from the resistance–strain curve of RGO network (Figure S14), but also possessed high electrical conductivity, which can be confirmed by serving as the conducting channels for LED bulb lighting (Figure 4d) due to the integrated structure of networks and excellent electrical conductivity of RGO fibers. The high electrical conductivity of the integrated 2D networks is ascribed to very low contact resistance at the *in situ* formed junctions, which we will mention. Directing writing technique can make 2D patterns not only at the bottom of the

coagulation bath, but also onto various substrates (*i.e.*, plastics, see Figure S15) if these substrates can be put into the coagulation bath. Programmable writing technique can make the resulting graphene-based networks with more complex structures, *i.e.*, spider web-like network as shown in Figure 4c.

Direct writing of the specific network patterns with GO inks has provided a very useful wet-technology to joint GO fibers together with *in situ* welded junctions. For instance, there are a lot of junctions, as shown in Figure 5a, formed during writing of the latitudinal and longitudinal fiber arrays in sequence at the bottom of the coagulation bath. Closer observation in one junction as shown in Figure 5b (and Figure S16) has indicated that there existed no obvious boundary between two different fibers in such a junction, which indicates that the latitudinal and longitudinal fibers have been welded together at the junctions after writing with the GO inks in the coagulation bath. Coagulating of the written structures and the subsequent drying process are probably the driving forces for such a very effective wet-welding. The joint points formed by *in situ* welded effect have made the GO networks with integral structures, which means that the integrated GO networks have possessed not only excellent mechanical property between perpendicular fibers, but also reasonable load transfer from one single fiber to entire network. To confirm the structural integrity of the resulting GO network, we have investigated the shear strength of the junction formed between two mutual perpendicular fibers in the network. As shown in Figure 5c, both ends of the junction in the lateral fiber were fixed by the glue and the longitudinal fiber is drawn by the external load. As shown in Figure 5d, the junction of GO fibers assembled by large size GO sheets (G-GOF) has shear strength of 11.2 MPa, higher than that (5.7 MPa) of GO fibers assembled by small size GO sheets (S-GOF) as the former possesses less defects, which is beneficial to the mechanical strength of the resulting fibers and junctions. After chemical reduction with hydroiodic acid, the shear strengths of the junctions assembled by large and small sheets are 15.7 and 7.9 MPa, respectively. These values are higher than those before reduction as the reduction process has resulted in the more compacted packing density of the 2D sheets.[40] The broken junction was recorded by digital camera and scanning electron microscopy as shown in Figure 5e and f, respectively, from which we can see that the rapture locates near the junction point of the lateral fiber rather than the junction point itself, which indicates that sufferable shear force of the junction is at least twice as high as that of the fiber, as two ends of the fiber have undertaken the shear force simultaneously.

CONCLUSION

Nonwoven, nonknitted, and flexible GO 2D networks with high mechanical performance have been fabricated by using programmable writing of the GO inks from the moveable spinneret along the designed tracks, and subsequently converted into the corresponding RGO networks with excellent electrical conductivity as well as enhanced mechanical properties by the thermal or chemical reduction process. The *in situ* welded junctions formed during aging and drying of the spun fibers have made the resulting networks with the integral structure, and outstanding mechanical properties together with excellent electrical conductivities have provided a great opportunity to sense the external mechanical stimuli of the spun fibers and their web integrations by using the electrical signals. The resulting GO and RGO 2D networks might find various emerging applications in many fields including electronic textiles.

METHODS

Synthesis of GO Sheets with Different Sizes. Large GO sheets with average lateral sized of 30 μm were synthesized from expanded graphite (CX-200, Qingdao Tianheda Graphite Co., Ltd., Qingdao, China.) by a modified Hummers' method.[11,43] To obtain GO sheets with various sizes, ultrasonication was used to process the large GO sheets synthesized above and the GO sheets with the average lateral size of 17 μm were obtained by 2 min sonicating with a Branson Digital Sonifier (S450D, 30% amplitude).

Direct Writing of GO Fibers. Two GO spinning dopes (30 and 17 μm) with the same viscosity (50 Pa·s) were injected into the stationary coagulation bath (200 μL/min). The injector moved back and forth at a rate of ~3 cm/s. The chosen coagulation bath was ethanol/water (1:1 v/v) solution with 0.4 wt % CTAB. After 30 min of immersion in coagulation bath, the GO gel fibers were transferred into the water and ethanol bath to wash away the residual coagulation solution, and the washed GO fibers were collected onto the bracket. The resulting products were dried at room temperature in air for 12 h and then dried at 60 °C under vacuum for 12 h again.

Direct Writing of GO Networks. The GO network in the spinning process was realized by adjusting the positions of the nozzle horizontally and vertically, which was carried out in the coagulation bath of 0.05 wt % CTAB. The use of CTAB in such a quite low concentration at this step is to avoid rapid solidification of single fibers. Then, the as-prepared GO network was transferred into deionized water for 5 min and into 0.4 wt % CTAB for 30 min in sequence. After washing off the residual coagulation solutions mentioned above, the GO network was obtained. The resulting products were dried at room temperature in air for 12 h and then dried at 60 °C under vacuum for 12 h again.

Conversion of the GO Fibers and Their Networks. Dried GO fibers and networks were immersed into the 45% hydriodic acid solution at 80 °C for 12 h. After the sample cooled to room temperature, both fibers and networks were washed with water and ethanol in sequence and dried at 100 °C under vacuum for 12 h. Through this chemical reduction process, both RGO fibers and networks were obtained.

Characterization. The SEM images were taken on a Hitachi S4800 field-emission SEM system with the acceleration voltage of 5 kV and Quanta 400 FEG field-emission SEM system with the acceleration voltage of 10 kV. The AFM observations were performed with a Dimension 3100 in the tapping mode. The samples for AFM observations were prepared by spin-coating of

diluted alcoholic dispersion of GO onto freshly exfoliated mica substrate at 500 rpm. The viscosity of GO solutions was measured using a NDJ-9SN precision viscometer (speed 6/12/30/60 rpm, range (10−1) × 10^5 mPa·s) purchased from Shanghai Precision and Scientific Instrument Corporation, Shanghai, China. The electrical properties were measured using standard four-probe method with an electrical measurement system connecting with a Keithley 2400 multifunctional source-meter and a Lakeshore low temperature system. The electromechanical stability of RGO fibers was test by a homemade two-point bending device (as shown in Figure 3a), where the radius of curvature was set to 3 cm and the bend speed was about one cycle per 50 s. Tensile tests were conducted using an MTS Nano Bionix Universal Testing System. The samples were mounted on paper tabs with a gauge length of 7 ± 1 mm. The extension speed was 0.001 mm/s. The phase composition was characterized by a Bruker D8 Advance X-ray diffractometer equipped (XRD) with Cu Kα radiation generator (0.151 nm, 40 kV, 40 mA) and Raman spectra with a Renishaw RM3000 Raman microscope (laser: 514 nm with a 2 μm spot size).

Conflict of Interest: The authors declare no competing financial interest.

Acknowledgment. This work was financially supported by the Natural Science Foundation of Jiangsu Province (No. BK20131172), the National Natural Science Foundation of China (No. 21373024, No. 51202282 and No. 21273269) and the 100 Talents Program of the Chinese Academy of Sciences.

Supporting Information Available: Viscosity *versus* concentration curves of the resulting GO dispersions, SEM images of the GO fibers with different diameters, EDX spectra of the GO/RGO fiber sampled at the top surface and cross section, digital photos showing free-standing RGO network with excellent flexibility, the digital photo of the GO network written on the PET substrate. This material is available free of charge *via* the Internet at http://pubs.acs.org.

REFERENCES AND NOTES

1. Cherenack, K.; van Pieterson, L. Smart Textiles: Challenges and Opportunities. *J. Appl. Phys.* **2012**, *112*, 091301-1–091301-14.
2. Park, S.; Jayaraman, S. Smart Textiles: Wearable Electronic Systems. *MRS Bull.* **2003**, *28*, 585–591.
3. Köhler, A. R. Challenges for Eco-Design of Emerging Technologies: The Case of Electronic Textiles. *Mater. Des.* **2013**, *51*, 51–60.
4. Bedeloglu, A. C.; Demir, A.; Bozkurt, Y.; Sariciftci, N. S. A Photovoltaic Fiber Design for Smart Textiles. *Tex. Res. J.* **2010**, *80*, 1065–1074.
5. Hu, L.; Pasta, M.; Mantia, F. L.; Cui, L.; Jeong, S.; Deshazer, H. D.; Choi, J. W.; Han, S. M.; Cui, Y. Stretchable, Porous, and Conductive Energy Textiles. *Nano Lett.* **2010**, *10*, 708–714.
6. Chen, T.; Qiu, L.; Yang, Z.; Cai, Z.; Ren, J.; Li, H.; Lin, H.; Sun, X.; Peng, H. An Integrated "Energy Wire" for both Photoelectric Conversion and Energy Storage. *Angew. Chem.* **2012**, *51*, 11977–11980.
7. Rattfält, L.; Lindén, M.; Hult, P.; Berglin, L.; Ask, P. Electrical Characteristics of Conductive Yarns and Textile Electrodes for Medical Applications. *Med. Biol. Eng. Comput.* **2007**, *45*, 1251–1257.
8. Huang, C.-T.; Shen, C.-L.; Tang, C.-F.; Chang, S.-H. A Wearable Yarn-Based Piezo-Resistive Sensor. *Sens. Actuators, A* **2008**, *141*, 396–403.
9. Cochrane, C.; Koncar, V.; Lewandowski, M.; Dufour, C. Design and Development of a Flexible Strain Sensor for Textile Structures Based on a Conductive Polymer Composite. *Sensors* **2007**, *7*, 473–492.
10. Geim, A. K.; Novoselov, K. S. The Rise of Graphene. *Nat. Mater.* **2007**, *6*, 183–191.
11. Zhu, Y.; Murali, S.; Cai, W.; Li, X.; Suk, J. W.; Potts, J. R.; Ruoff, R. S. Graphene and Graphene Oxide: Synthesis, Properties, and Applications. *Adv. Mater.* **2010**, *22*, 3906–3924.
12. Neto, A. C.; Guinea, F.; Peres, N.; Novoselov, K. S.; Geim, A. K. The Electronic Properties of Graphene. *Mod. Phys.* **2009**, *81*, 109.
13. Lee, C.; Wei, X.; Kysar, J. W.; Hone, J. Measurement of the Elastic Properties and Intrinsic Strength of Monolayer Graphene. *Science* **2008**, *321*, 385–388.
14. Balandin, A. A. Thermal Properties of Graphene and Nanostructured Carbon Materials. *Nat. Mater.* **2011**, *10*, 569–581.
15. Liu, M.; Yin, X.; Zhang, X. Double-Layer Graphene Optical Modulator. *Nano Lett.* **2012**, *12*, 1482–1485.
16. Huang, X.; Zeng, Z.; Fan, Z.; Liu, J.; Zhang, H. Graphene-Based Electrodes. *Adv. Mater.* **2012**, *24*, 5979–6004.
17. Huang, X.; Qi, X.; Boey, F.; Zhang, H. Graphene-Based Composites. *Chem. Soc. Rev.* **2012**, *41*, 666–686.
18. Huang, X.; Yin, Z.; Wu, S.; Qi, X.; He, Q.; Zhang, Q.; Yan, Q.; Boey, F.; Zhang, H. Graphene-Based Materials: Synthesis, Characterization, Properties, and Applications. *Small* **2011**, *7*, 1876–1902.
19. He, Q.; Wu, S.; Yin, Z.; Zhang, H. Graphene-Based Electronic Sensors. *Chem. Sci.* **2012**, *3*, 1764–1772.
20. Marcano, D. C.; Kosynkin, D. V.; Berlin, J. M.; Sinitskii, A.; Sun, Z.; Slesarev, A.; Alemany, L. B.; Lu, W.; Tour, J. M. Improved Synthesis of Graphene Oxide. *ACS Nano* **2010**, *4*, 4806–4814.
21. Sui, Z.; Zhang, X.; Lei, Y.; Luo, Y. Easy and Green Synthesis of Reduced Graphite Oxide-Based Hydrogels. *Carbon* **2011**, *49*, 4314–4321.
22. Stankovich, S.; Dikin, D. A.; Piner, R. D.; Kohlhaas, K. A.; Kleinhammes, A.; Jia, Y.; Wu, Y.; Nguyen, S. T.; Ruoff, R. S. Synthesis of Graphene-Based Nanosheets *via* Chemical Reduction of Exfoliated Graphite Oxide. *Carbon* **2007**, *45*, 1558–1565.
23. Chen, Z.; Ren, W.; Gao, L.; Liu, B.; Pei, S.; Cheng, H.-M. Three-Dimensional Flexible and Conductive Interconnected Graphene Networks Grown by Chemical Vapour Deposition. *Nat. Mater.* **2011**, *10*, 424–428.
24. Li, X.; Sun, P.; Fan, L.; Zhu, M.; Wang, K.; Zhong, M.; Wei, J.; Wu, D.; Cheng, Y.; Zhu, H. Multifunctional Graphene Woven Fabrics. *Sci. Rep.* **2012**, *2*, 395.
25. Cao, X.; Shi, Y.; Shi, W.; Lu, G.; Huang, X.; Yan, Q.; Zhang, Q.; Zhang, H. Preparation of Novel 3D Graphene Networks for Supercapacitor Applications. *Small* **2011**, *7*, 3163–3168.
26. Dong, Z.; Jiang, C.; Cheng, H.; Zhao, Y.; Shi, G.; Jiang, L.; Qu, L. Facile Fabrication of Light, Flexible and Multifunctional Graphene Fibers. *Adv. Mater.* **2012**, *24*, 1856–1861.
27. Xiang, C.; Young, C. C.; Wang, X.; Yan, Z.; Hwang, C. C.; Cerioti, G.; Lin, J.; Kono, J.; Pasquali, M.; Tour, J. M. Large Flake Graphene Oxide Fibers with Unconventional 100% Knot Efficiency and Highly Aligned Small Flake Graphene Oxide Fibers. *Adv. Mater.* **2013**, *25*, 4592–4597.
28. Xu, Z.; Gao, C. Graphene Chiral Liquid Crystals and Macroscopic Assembled Fibres. *Nat. Commun.* **2011**, *2*, 571.
29. Compton, O. C.; Nguyen, S. T. Graphene Oxide, Highly Reduced Graphene Oxide, and Graphene: Versatile Building Blocks for Carbon-Based Materials. *Small* **2010**, *6*, 711–723.
30. Li, D.; Mueller, M. B.; Gilje, S.; Kaner, R. B.; Wallace, G. G. Processable Aqueous Dispersions of Graphene Nanosheets. *Nat. Nanotechnol.* **2008**, *3*, 101–105.
31. Park, S.; An, J.; Piner, R. D.; Jung, I.; Yang, D.; Velamakanni, A.; Nguyen, S. T.; Ruoff, R. S. Aqueous Suspension and Characterization of Chemically Modified Graphene Sheets. *Chem. Mater.* **2008**, *20*, 6592–6594.
32. Zou, J.; Kim, F. Self-Assembly of Two-Dimensional Nanosheets Induced by Interfacial Polyionic Complexation. *ACS Nano* **2012**, *6*, 10606–10613.
33. Cong, H. P.; Ren, X. C.; Wang, P.; Yu, S. H. Wet-Spinning Assembly of Continuous, Neat, and Macroscopic Graphene Fibers. *Sci. Rep.* **2012**, *2*, 613.
34. Chen, L.; He, Y.; Chai, S.; Qiang, H.; Chen, F.; Fu, Q. Toward High Performance Graphene Fibers. *Nanoscale* **2013**, *5*, 5809–5815.
35. Xu, Z.; Sun, H.; Zhao, X.; Gao, C. Ultrastrong Fibers Assembled from Giant Graphene Oxide Sheets. *Adv. Mater.* **2013**, *25*, 188–193.

36. Hearle, J. W. *High-Performance Fibres*; Woodhead Publishing: Cambridge, England, 2001; Vol. 15.
37. Wang, X.; Bai, H.; Shi, G. Size Fractionation of Graphene Oxide Sheets by pH-Assisted Selective Sedimentation. *J. Am. Chem. Soc.* **2011**, *133*, 6338–6342.
38. Thilly, L.; Lecouturier, F.; Von Stebut, J. Size-Induced Enhanced Mechanical Properties of Nanocomposite Copper/Niobium Wires: Nanoindentation Study. *Acta. Mater.* **2002**, *50*, 5049–5065.
39. Jalili, R.; Aboutalebi, S. H.; Esrafilzadeh, D.; Shepherd, R. L.; Chen, J.; Aminorroaya-Yamini, S.; Konstantinov, K.; Minett, A. I.; Razal, J. M.; Wallace, G. G. Scalable One-Step Wet-Spinning of Graphene Fibers and Yarns from Liquid Crystalline Dispersions of Graphene Oxide: Towards Multifunctional Textiles. *Adv. Funct. Mater.* **2013**, *23*, 5345–5354.
40. Pei, S.; Cheng, H.-M. The Reduction of Graphene Oxide. *Carbon* **2012**, *50*, 3210–3228.
41. Xu, Z.; Liu, Z.; Sun, H.; Gao, C. Highly Electrically Conductive Ag-Doped Graphene Fibers as Stretchable Conductors. *Adv. Mater.* **2013**, *25*, 3249–3253.
42. Wichmann, M. H.; Buschhorn, S. T.; Böger, L.; Adelung, R.; Schulte, K. Direction Sensitive Bending Sensors Based on Multiwall Carbon Nanotube/Epoxy Nanocomposites. *Nanotechnology* **2008**, *19*, 475503.
43. Hummers, W. S., Jr.; Offeman, R. E. Preparation of Graphitic Oxide. *J. Am. Chem. Soc.* **1958**, *80*, 1339–1339.